Insights into the Position of Kyrgyzstan in the Silurian

by

Syamil Razak

Submitted as an Honors Thesis

Department of Earth and Environmental Sciences

The University of Michigan

April 2013

Accepted by

[signature]	R. VAN DER VOO	April 19, 2013
Signature	Name	Date
Signature	Name	Date

ACKNOWLEDGEMENT

First and foremost, I would like to extend my most heart-felt appreciation and gratitude to my advisor, Dr. Rob Van der Voo for the knowledge and wisdom that he had shared, for the guidance in times of confusion and for the support and encouragement in times of despair. His patience, dedication and undivided attention has not only made this thesis possible, but has also inspired me beyond this research experience. I also would like to thank ex-graduate student, Ada Dominguez who has answered my plethora of questions and has patiently taught me how to use all of the instruments in the lab. In addition, my thank you goes to Professor Philip Gingerich for reviewing this thesis in spite of his very busy schedule.

I also would like to thank the entire paleomagnetism team, Zach Menzo, Drew Biebuyck, Sam Nemkin, Fatim Hankard, Matt Domeier and Ethan Hyland for the knowledge that has been shared in the past 2 years. I thank everybody who has helped me with this thesis, directly or indirectly and I am very grateful to be reminded constantly that learning is a life-long process and everybody is a teacher and a learner. Thank you.

ABSTRACT

This study examined 101 cores from 16 basaltic flows from the Silurian in northern Kyrgyzstan with the aim of understanding the paleoposition of Kyrgyzstan. This is important as very little is known about the Kazakhstania terranes which comprises Kyrgyzstan in the early to middle Paleozoic. The result of this study may help us understand the amalgamation process of the island arcs and microcontinents that were thought to have joined together in the Ordovician.

The magnetic behavior of the cores from this collection seems to suggest that both hematite and low-titanium magnetite are present as the magnetic carrier. Characteristic magnetization is carried by low-titanium magnetite while secondary magnetization is prominent and carried by hematite. The magnetic behavior of samples with hematite could reflect ancient magnetic directions but are poorly clustered. In contrast, samples with magnetite show steep magnetic directions that resemble Cenozoic magnetizations.

To increase accuracy and credibility of the data, visual inspection and reliability criteria of *Van der Voo (1990)* were used to filter highly erroneous samples. Overall formation mean of the study sites gave paleomagnetic directions that are southerly and up and northerly and down. Scattered directions are present owing to undefined folding events and complicated tectonic history in the study area.

U-Pb radiometric age analysis of zircon from the basalt revealed an age of 423 ± 5.4Ma with a confidence level of 96.1%. The expected direction from volcanic rocks of this locality is not steep if the age is Silurian; however this study has obtained both steep and shallow directions with noisy behavior in thermal demagnetization and failing a fold test. We attribute this disappointing remanence to late-stage alteration. By considering only characteristic magnetic directions, the final mean of site directions was calculated to have declination and inclination of 181.7° and -86.6° respectively with the $\alpha 95$ of 12.3° which does not agree with an expected direction of Silurian age.

INTRODUCTION

The directions and intensity of the ancient Earth's magnetic field are recorded in magnetic minerals present in volcanic rocks, and are typically, but not always, acquired at the time of cooling. On average, shifts in orientation and intensity happen every ~400,000 years and are recognizable with a magnetic compass. While the geographic north of the Earth is static, the magnetic north shows polarity reversals and apparent polar wander due to this shift. Records have shown that every five years, the declination changes up to 1°. The changes in magnetic intensity and inclination sign together with the apparent polar wander path as a result of the change in the location of the magnetic north are called secular variation.

These occurrences were first realized when geologists discovered that some volcanic rocks are magnetized in a direction that is opposite to the present day magnetic field. The magnetic field of the earth switches between periods of normal and reverse polarity and as of today we live in the former direction. Intervals of a given polarity are referred to as chrons. The study of paleomagnetism is only made possible by a magnetometer that measures the direction and intensity of the remanent magnetic minerals in volcanic rocks, and thereby can monitor the changes in polarity and in apparent polar wander.

The reason behind secular variation is the instability of the Earth's dynamo, manifested in the patterns in the changes of secular variation. Due to gradual cooling, the inner core of the Earth grows in size and consequently, the liquid outer core decreases in size. This is hypothesized to affect the intensity and polarity of the magnetic field generated by the dynamo. In addition, higher order magnetic fields should also be considered. Although paleomagnetic records of volcanic rocks dating from early Paleozoic have shown dominance of main dipolar field, octupoles or quadrupoles field of varying intensity may have long-term contributions.

With the advances in radiometric dating methodologies and global sampling efforts, worldwide paleomagnetic data are combined to aid understanding of the spatiotemporal locations of continents under the assumption that the magnetic field averaged out to be dipolar. However, due to variations over time, some geologic periods may have experienced a higher contribution of non-dipole fields. Therefore, further understanding on the inner workings of the Earth is essential in making continental reconstructions. Furthermore, due to tectonic activities and weathering, the paleomagnetic data from early Paleozoic are often not as complete and accurate as data from younger periods.

In this study, a collection of volcanic rocks from basaltic flows in northern Kyrgyzstan were demagnetized and analyzed to obtain the magnetic directions and eventually a paleomagnetic pole. The paleopole of the area that resembles the total ancient geomagnetic field is then calculated from magnetic directions of reliable sampling sites. However, it is worth noting that VGPs and paleopole are calculated with a dipole formula without consideration of higher order components.

GEOLOGICAL SETTING

The sampling area is located in northern Kyrgyzstan at GPS coordinates of 42.5°N and 72.5°E **(Figure 1)**. All 16 sites sampled are composed largely of volcanic rocks intertwined with conglomerates and sandstones. Most sites are nearly flat-lying and have turned reddish-brown from black due to weathering. The basaltic layers found at each sites are mafic in nature and are separated from each other by layers of greenish sandstone. Most of the sandstone layers have been eroded and have products of erosion. The thicknesses of the basaltic layers vary between 100-250m with different bedding orientations that suggest post-depositional tectonic activities.

As determined by U-Pb dating method, the layers are found to be of the Silurian age at approximately 432 ±5.4Ma *(Joe Meert, personal communication)*. A long history of deformation is associated with the

sampling area due to the Devonian volcanic arc that forms an oroclinal bending in Kazakhstan *(Van der Voo, 2004)* and the assembly of Asia in late Paleozoic. Two separate views of the assembly mechanism of the area have been introduced. The first view suggests the collision of microcontinents separated by oceanic basins and island arcs *(Filippova et al., 2001; Windley et al., 2007)* while the second view suggests an oroclinal bending of a single long-lived subduction system *(Şengör and Natal'in, 1996).*

Throughout the Silurian up to Early Permian, the tectonic activities are marked by volcanic margins in the blocks that were amalgamated to form "Kazakhstania" *(Skrinnik and Horst, 1995)*. **Figure 1a** shows the schematic map of central Asia and the sampling location is marked with a filled red circle. The sampled rocks in this collection are basaltic in nature and occurred along the south-west boundary of the outcrops of Precambrian metamorphic rocks *(Abdullin et al., 1980)*. As such, the sampling area falls in the Late Paleozoic Chu-Sarysu sedimentary basin formed at the margin of Precambrian rocks **(Figure 1b)**.

This sampling area was selected as it will provide directional information that will ultimately lead to the knowledge of the paleoposition of Kyrgyzstan in the Silurian. Since the sites are located just outside the orocline, this study, given reliable paleomagnetic and age-dating results, will help us further understand the amalgamation process of Kazakhstania. It has been established that rocks on the inside of the orocline are younger than rocks found on the outer side of the orocline. Comparison of magnetic directions of the study area in the Silurian and of younger surrounding rocks will provide snapshots of the movement sequences of cratons as the basaltic layers were deposited and magnetic directions were gained during the tectonic processes.

SAMPLING METHODS

In this study, 101 individual samples were collected from 16 basaltic flows in northern Kyrgyzstan by Ada Dominguez in the summer of 2011. The sites are numbered from 61 to 76 whereas collections from site 1 through 60 are being studied by Dr. Mikhail Bazhenov's paleomagnetism team in Russia. Only a small proportion of the samples were drilled with a portable Pomeroy drill as the equipment became dysfunctional at the beginning of the sampling trip. Most of the cores were drilled in the lab from hand samples. The strike and dip of the hand samples were measured with a compass and the azimuth and the plunge of the cores were determined using a Brunton compass, or a solar compass whenever there is a strong magnetic influence in the field and weather is permitting.

The hand samples were leveled and casted in plaster of Paris before being drilled into standard 2.5cm diameter cylindrical cores. The azimuths of the cores were marked with the arrows pointing in the down direction. The cores then were cut to a 2.5cm height with diamond-tipped saw and rust stains were washed way. Each sample was let to dry and then marked with non-magnetic and temperature resistant paint. The hand samples that were brought in were weathered and some were friable; any broken specimens were cemented with alumina cement that will not affect the magnetic readings of the magnetometer.

Geographic location and bedding orientation of the sites were recorded (see Appendix). Whenever possible, only fresh outcrops were sampled to reduce the effects of weathering. Lightning prone areas were avoided to reduce the risk of secondary remagnetization due to lightning. The flows were overlapping but the thicknesses of approximately 150m each allowed sampling in the middle column of the flow to avoid any baked contact effects. Due to the basaltic nature of the flows and the presence of small zircon minerals, it is assumed that the cooling of the flows happened at a fast rate and the magnetization recorded is acquired at cooling time.

The declination deviation for the sampling area was calculated with the National Geophysical Data Center (NGDC) calculator from the United States National Oceanic and Atmospheric Administration (NOAA) using the latitude 42°N and 72°E for July 2011when the sampling effort was made. A deviation value of 5.2°E was given and is to be added to the azimuth of the sample's field orientation and declination. **Table 1** lists magnetic properties for each sample in ascending order (from sample 291-346) and **Table 2** lists magnetic properties for each site obtained by Fisherian statistics in ascending order (from site 61-76). **Table 4** shows the magnetic properties for each site obtained with the great circle analysis. All values in the three tables were left un-corrected of declination correction, but this will be done when the collection of Dr. Bazhenov and ours are merged.

LABORATORY METHODS

Measurements of natural remanent magnetization (NRM) and its behavior in thermal demagnetization were conducted in a magnetically shielded room in the Paleomagnetism, Structure and Tectonics Laboratory (PaSTeL) at the University of Michigan to avoid magnetic contamination by viscous magnetization in the samples. The magnetic intensities and directions were measured with a three-axis 2G superconducting magnetometer. Alternating field demagnetization was not conducted on the samples from this collection but all of them were thermally demagnetized at small temperature steps using an ASC TD-48 demagnetizer located in the shielded room with a residual field of < 200nT.

Results of demagnetization treatments were plotted in orthogonal vector diagrams *(Zijderveld, 1967)* and in stereographic projection. For quantitative and statistical analyses on the magnetic directions, principle component analysis (PCA) (Kirschvink, 1980) was used on linear segments of the Zijderveld plot. Whenever stable endpoints were not obtained, a combined analysis of remagnetization circles seen

as forming a great circle path and stable endpoints observations was used *(McFadden & McElhinny, 1988).* Paleomagnetic measurements were analyzed using Paleomac software *(Cogné, 2003).*

DIRECTIONAL ANALYSIS

Most analyzed samples in this collection show noisy univectorial decay to the origin with MAD angle between 2.2°-16.6° **(Table 1)**. A good decay would exhibit a MAD angle value of < 3°, therefore half of the samples in this collection are on the lower quality end. Low temperature overprints are generally removed at ~250°Celcius. **Figures 2-6** show stereonet, intensity diagram and Zijderveld plot for 5 different samples from different sites. In **Figure 2**, we have observed a sharp decrease in magnetic intensity between 100-300° Celcius indicating the presence of a low unblocking temperature component such as titanomagnetite or goethite.

For most of the samples, an unblocking temperature of 580° Celcius is observed indicating that magnetite is responsible as the main carrier for the higher temperature component of the magnetic direction **(Figure 5).** Some samples **(Figures 4, 6)** indicate the presence of hematite probably due to the oxidation of original magnetite. The directions of the hematite components are different from those of the magnetite components indicating that they are new minerals made secondarily, or perhaps even during the thermal demagnetization process.

FOLD TEST

Sampling of basaltic flows with different bedding orientation was done to allow a fold test (see Appendix for bedding orientation). As the sampling area has been subjected to continuous deformation since the deposition of the flows, this test is necessary to check whether a magnetization was acquired before, during or after the folding. According to Graham (1949) if a region was magnetized prior to

folding then the magnetic directions will become more clustered when restored to horizontal. For post-folding magnetization, the opposite is true.

For this collection, a fold test was done to determine whether the magnetization predates the deformation. **Table 3** shows all the magnetic directions used in this test. Due to the high α95 of the site means obtained through Fisherian statistics, magnetic directions of individual samples were used instead of site means to avoid the misrepresentation of data. Sample directions, both in-situ and tilt-corrected were plotted **(Figure 8).** Both stereonets were visually compared and no significant change in scatter was observed, indicating an inconclusive fold test. In general, the directions of the samples from this sampling area are scattered and these deviations are present across all samples. The fold test is statistically inconclusive at the 95% confidence level with a k-ratio of 0.79 (k2/k1, **Table 3**) using the method of *McElhinny (1964).*

RELIABILITY CRITERIA

In order to successfully come up with a strong conclusion, samples used must satisfy a set of reliability criteria. In this paper, we will use a set of seven criteria as suggested by *Van der Voo (1990).* The ages of the basalts from the sampling area in northern Kyrgyzstan are well determined through U-Pb radiometric dating method on zircons found in the basalts. An age of 432 ±5.4Ma was obtained **(Figure 11)** but the magnetization of the rocks may not have the same age as the rock itself given the fold test, failing criterion 1.

Although the second criterion appears satisfied by having 101 samples from which statistical parameters, *α95* and *k* are drawn, the low k-values (**Table 3**, $k \leq 10$) make this results fail criterion 2. Most of the site means obtained through Fisherian statistics yields unsatisfactory values of *α95* and *k* **(Table 2),** however improved values of *α95* **(Table 4)** were obtained through the great circle analysis.

Both Fisherian and great circle analysis **(Figure 7, Figure 10)** yield similar mean direction across all sites.

The samples in this collection were thermally demagnetized and most samples show noisy univectorial decay with MAD angles from 2.2° to 16.6°, satisfying criterion 3. Stable presumably primary magnetic directions were plotted on stereonet and orthogonal vector diagrams *(Zijderveld, 1967)* were used with Principal Component Analysis *(Kirschvink, 1980)* to identify the primary vector of magnetic directions. To identify the presence of different magnetic carriers, thermal demagnetization steps are set to the small enough to detect different vector components. Criterion 4, requiring fold test or contact test if appropriate is not satisfied. As already mentioned, the fold test is negative, or at best, inconclusive.

The sampling area is located in northern Kyrgyzstan, just southwest of Lake Balkhash in close proximity to the Ural-Mongol fold belt *(Collins, 2003)* within the Central Asia Orogenic Belt. Criterion 5 requires structural control and tectonic coherence with the block involved, however controversies about the regional tectonics are present and there is no guarantee that the sampling area has not been affected by tectonic rotation since the deposition of the basaltic layers in the Silurian. Even after applying bedding corrections, samples show noisy directions and poor clustering, indicative of complex tectonic processes that require a more detailed study.

From the directions observed in this collection, we have recorded both normal and reverse polarities, satisfying criterion 6. Remagnetization however is likely due to the age of the rocks and the nature of the formation which was weathered. In this collection, stable decay is observed to be carried by magnetite, however the scattering in magnetic directions of samples have induced doubts whether the directions are entirely primary.

PALEOMAGNETIC SITE MEANS & MEAN POLES

In this study, site means are obtained through Fisherian analysis **(Table 2)** and great circle analysis **(Table 4).** In Fisherian analysis, the mean for each site is computed using spherical statistics. The α95 of site means generally are large due to the scattering in magnetic directions recorded by the samples. Only individual samples that have α95 <18° are considered in the calculation of site means. Using the first method, a reverse polarity direction with declination of 181.7°, inclination of -86.6° and α95 of 17.1 is obtained **(Figure 7)**.

With the great circle analysis **(Table 4)**, a best fit plane for the decay path of the magnetization in each sample is calculated. The normals for each of these planes lie on a great circle and the normal to the latter great circle represents the magnetic direction in common to all sites. **Figure 10** shows two stereonets; one with the best fit planes that correspond to each site and the second depicting the normal to these planes and the great circle formed with these normals. The closed square in the stereonet represents a common direction that has a declination of 163°, inclination of 80.8° and α95 of 22.7.

The two analyses came to a similar conclusion on the steepness of the mean of the magnetic direction. According to the obtained results, during the Silurian, the study area was situated near the polar region with inclination ±80.8°.This observed direction does not agree with the magnetic directions obtained from previous studies of Devonian and Silurian rocks from the region. This will be discussed in the next section.

The low temperature component of all the samples shows scattering in magnetic direction and does not resemble present day magnetic field. This may suggest that an imprint of magnetic direction younger than Silurian but older than present day field has affected the paleomagnetic results. The VGP of each site was calculated and can be seen in **Table 2**. The high α95 value of the mean magnetic direction

of each site propagates into the VGPs and leads to high values of dp and dm. The sites VGPs were plotted on an orthographic projection diagram **(Figure 9)** and using Fisherian analysis, the mean pole was calculated to have a Pole Longitude: 268.8°, Pole Latitude: -83.2° and α95: 28.2°.

RESULTS & DISCUSSION

The main goal of this study is to refine the paleoposition of Kyrgyzstan in the Silurian to further understand the amalgamation process of Kazakhstania and to gain more insights into the tectonic episodes that led to the Devonian orocline in present day Kazakhstan. The study area is located to the west of the orocline and the rocks sampled are of basaltic flows at the margin of micro-continental blocks. To tighten the constraint of this study, we have assumed that the volcanic activity happened due to subduction and the movement of island arcs and micro-continents that ultimately formed the orocline in the Devonian, as part of the central Asia orogenic belt. A radiometric dating has further tightened the constraint by yielding an age of the basalts as 432 Ma with the U-Pb technique on zircons *(J.G.Meert, pers. comm., 2012);* See **Figure 11**. With this knowledge, it could be inferred that the landmass associated with the magnetic directions observed in this study reflects a Silurian paleoposition but alternative explanations need to be considered as well.

Site means observed in this study yield high values of α95 although the α95 values of individual samples are small. Both Fisherian analysis and great circle analysis agreed on a steep magnetic direction with a relatively large α95 values. It needs to be considered that the paleomagnetic results of this study may have been affected by episodes of alterations. As the inclination information provides a paleolatitudes estimate for the region, the magnetic directions observed in the Silurian rocks of this study pose a question as it does not agree with the previous results obtained from Silurian and Devonian rocks from the region. A study by *Abrajevitch (2007)* yields a magnetic declination and inclination of 106.5° and -46.4° of Devonian rocks involved in the orogenic process in the region. Studies by *Alexyutin et al*

(2007), Levashova et al (2003) and *Grishin et al (1997)* have yielded Silurian paleolatitudes from -1° to +13°. The average inclination obtained in this study is -86.6° yielding a paleolatitude estimate of +83.2° which is too steep to agree with previously published results.

In fact, this paleolatitude estimate is inexplicably higher than previously published Devonian paleolatitudes of the region. Recent study by *Levashova (2007)* estimates a value of +36° as the paleolatitude estimate for the region in Devonian. Considering the northward movement of the island arcs, terranes and microcontinents in the amalgamation process that ends in the Devonian, it is quite puzzling to infer this polar paleo-location observed from this study. Given our current understanding of the tectonic and spatial history of the region and the rate at which continents move, it is not acceptable to deduce that this study site has moved close to the North Pole and then back to the equatorial region in the Silurian.

As the paleolatitude estimate of the sampling site seems to agree with known Cenozoic paleolatitude estimate, we speculate that the characteristic magnetization carried by low-titanium magnetite may have been acquired as a result of exsolution of meta-stable titanomagnetite into its end-components. Having said this, the rocks sampled have shown characteristic magnetization of the Cenozoic and no estimation on Silurian paleolatitude can be made.

CONCLUSION

This study has obtained a rather steep magnetic direction for Silurian rocks of this locality. The mean magnetic direction observed has declination and inclination if 181.7° and -86.6° respectively with an α95 of 17.1°. 12 sites out of 16 were selected as they contain at least 3 promising individual samples with an α95 values of <17°. Both Fisherian statistic and great circle analysis were used to obtain a mean magnetic direction which has a steep inclination, resulting in an estimate for a high paleolatitude. The

characteristic magnetization of rocks in this collection is carried by low-titanium magnetite with unblocking temperature of lower than 580°Celcius. The magnetic carrier (low-titanium magnetite) may have grown during alteration by exsolution of titanomagnetite. A higher temperature secondary magnetization that imprints the steep primary direction is generally removed at > 580° Celcius. It shows highly scattered magnetic directions observed with unblocking temperature beyond 580°Celcius indicative of hematite. The hematite may have grown as new oxides introduced as a result of oxidation of magnetite during alteration.

The result of this study contribute very little to confirm or support the two prevailing theories on the assembly mechanism of the area, whether there was a single long-lived subduction system *(Şengör and Natal'in, 1996)* or collision of microcontinents separated by oceanic basins and island arcs *(Filippova et al., 2001; Windley et al., 2007).* These authors have agreed that by Early Permian, the amalgamation process has produced Kazakhstania. The study site is located on the outer side of the orocline, however the paleolatitude estimate that we have obtained in this study, +83.2° does not agree with any of the previously published results that claim a near-equatorial Silurian paleolatitude of -1° to +13°. A fold test was conducted with individual samples and an inconclusive result was obtained. Due to the nature of the sampling area that has been subjected to complicated tectonic history, a larger sampling size must be obtained in order to obtain a reliable paleoposition. Hopefully this study has been useful in improving our knowledge on the amalgamation process of Eurasia.

REFERENCES

Abdullin, A.A., Volkov, V.M., Scherba, G.N. 1980. (eds.) *Chu-Ili ore belt*. Nauka, Almaata, 503. (in Russian).

Abrajevitch, A.V., Van der Voo, R., Levashova, N.M., Bazhenov, M.L. 2007. *Paleomagnetism of the mid-Devonian Kurgasholak Formation, Southern Kazakhstan: Constraints on the Devonian paleogeography and oroclinal bending of the Kazakhstan volcanic arc*. Tectonophysics, 441:67–84.

Allen, M.B., Alsop, G.I., Zhemchuzhnikov, V.G. 2001. *Dome and basin refolding and transpressive inversion along the Karatau fault system, southern Kazakhstan*. Journal of Geological Society of London, 158:83-95.

Alexyutin, M.V., Bachtadse, V., Alexeiev, D.V., Nikitina, O.I. 2005. *Paleomagnetism of Ordovician and Silurian rocks from the Chu-Yili and Kendyktas Mountains, South Kazakhstan* . Geophysical Journal International, 162:321-331.

Cogné, J.P., 2003, *PaleoMac: A MacintoshTM application for treating paleomagnetic data and making plate reconstructions*. Geochemistry Geophysics Geosystems, 4:1-8.

Collins, A.Q., Degtyarev, K.E., Levashova, N.M., Bazhenov, M.L., Van der Voo, R. 2003. *Early Paleozoic paleomagnetism of east Kazakhstan: implications for paleolatitudinal drift of tectonic elements within the Ural-Mongol belt*. Tectonophysics, 377: 229-247.

Degtyarev, K. E. 2003. *The position of the Aktau-Junggar microcontinent in the Paleozoides of Central Kazakhst*an. Geotectonics. 37 (4):14-34.

Filippova, I.B., Bush, V.A., Didenko, A.N. 2001. *Middle Paleozoic subduction belts: The leading factor in the formation of the Central Asian fold-and-thrust belt*. Russian Journal of Earth Sciences, 3 (6):405–426.

Graham, J.W., 1949, *The stability and significance of magnetism in sedimentary rocks*. Journal of Geophysical Research, 54:131-167.

Grishin, D.V., Pechersky, D.M., and Degtyarev, K.E. 1997. *Paleomagnetism and reconstruction of Middle Paleozoic structure of Central Kazakhstan*. Geotectonics, 1:71– 81.

Kirschvink, J.L., 1980. *The least-square line and plane and the analysis of paleomagnetic data*. Geophysical Journal of the Royal Astronomical Society, 62:699– 718.

Levashova, N.M., Degtyarev, K.E., Bazhenov, M.L., Collins, A.Q., Van der Voo, R. 2003. *Middle Paleozoic paleomagnetism of east Kazakhstan: post-Middle Devonian rotations in a large-scale orocline in the central Ural–Mongol belt*. Tectonophysics, 377, 249–268.

Levashova, N.M., Mikolaichuk, A.V., McCausland, P.J.A, Bazhenov, M.L., Van der Voo, R. 2007. *Devonian paleomagnetism of the North Tien Shan: Implications for the middle-late Paleozoic paleogeography of Eurasia*, Earth and Planetary Science Letters, 257(1-2):104-120..

McFadden, P.L., McElhinny, M.W., 1988. *The combined analysis of remagnetization circles and direct observations in paleomagnetism*. Earth and Planetary Science Letters, 87:161-172.

Şengör, A.M.C., Natal'in, B.A. 1996. *Paleotectonics of Asia: fragments of a synthesis*. In: Yin, A., Harrison, M. (Eds.), The Tectonic Evolution of Asia. Cambridge Univ. Press, Cambridge. 486– 640.

Skrinnik, L.I., Horst, V.E. 1995. *Devonian island arc volcanic complexes in the Junggar Alatau*. Geology and exploration of Kazakhstan, 4: 6-10.

Van der Voo, R., 1990. *The reliability of paleomagnetic data*. Tectonophysics, 184:1-9.

Van der Voo, R. 2004. *Paleomagnetism, oroclines and the growth of the continental crust*. GSA Today, 14 (12):4-9.

Windley, B.F., Alexeiev, D., Xiao, W.J., Kröner, A., and Badarch, G. 2007. *Tectonic models for accretion of the Central Asian Orogenic Belt*. Journal of the Geological Society of London, 164:31-47.

Zijderveld, J.D.A., 1967. *AC demagnetization of rocks: analysis of results*. In: Collinson, D.W., Creer, K.M. (Eds.), Methods in Paleomagnetism. Elsevier, Amsterdam, 254– 286.

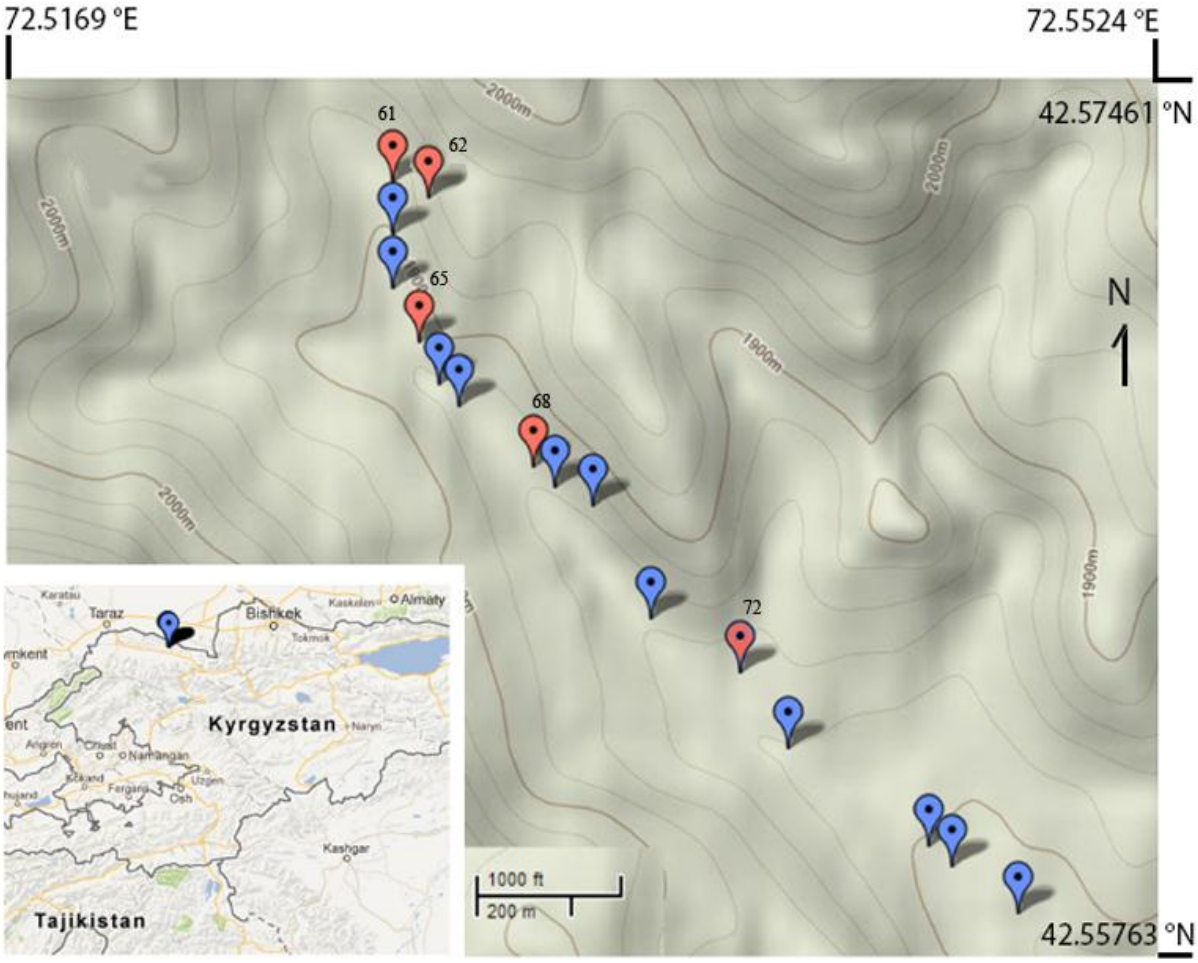

Figure 1: Map of the sampled region with contour lines. The blue and red pins indicate sampled sites. Sites labeled with blue pins were used in the calculation for paleopole. The sites labeled with red pins were not used as they did not satisfy reliability criteria by *Van der Voo (1990).* Sites that were selected has to have an N3 (number of individual samples used for analysis) of at least 2. Individual samples with α95 value of >17° are disqualified. The inset on the lower left shows the location of the sampled area. All images were adapted from *GoogleMaps.*

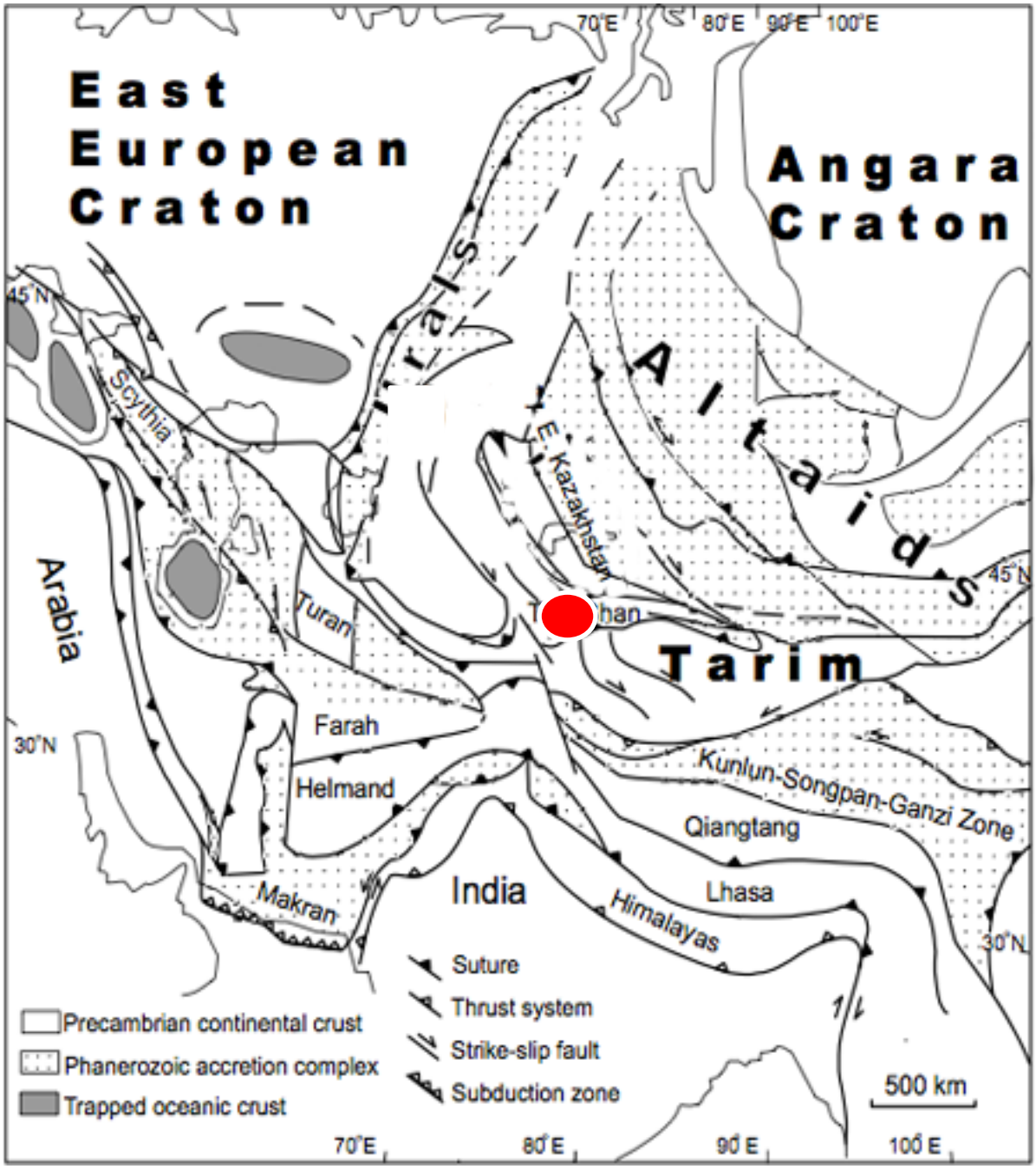

Figure 1.a: Schematic map of central Asia, showing the location of the sampling area as marked with the filled red circle, wedged between Baltica, Siberia and Tarim cratons. Adapted from *Allen et al., 2001*.

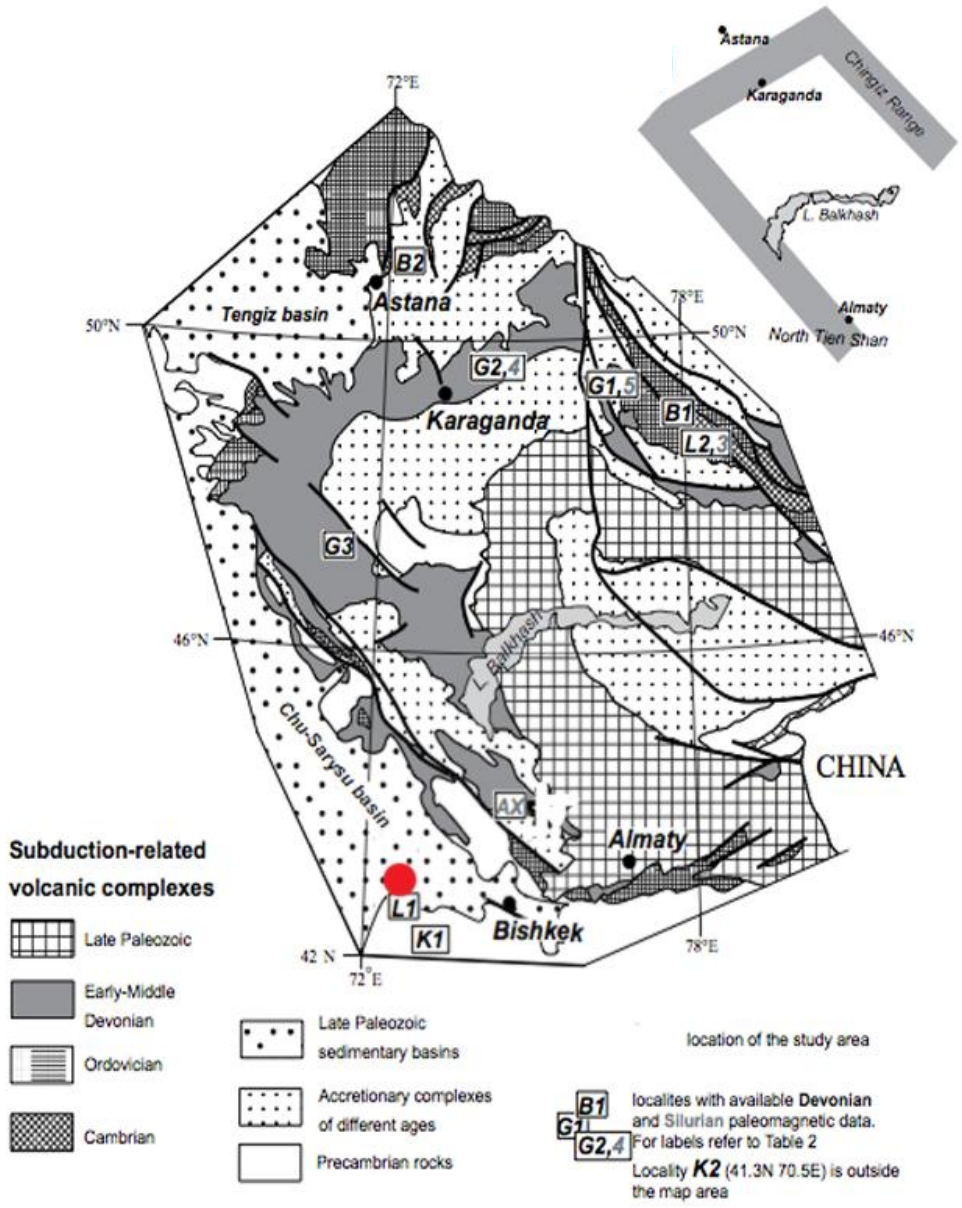

Figure 1.b: Paleozoic subduction related complexes in central Asia. A curved Devonian and late Paleozoic volcanic belts are shown with North Tien Shan at the lower end and Chingiz Range at the upper end. Previously published Silurian and Devonian paleomagnetic results are also indicated. Sampling site is shown as a filled red circle on the figure. Adapted from *Abrajevitch, 2008* and *Degtyarev, 2003*.

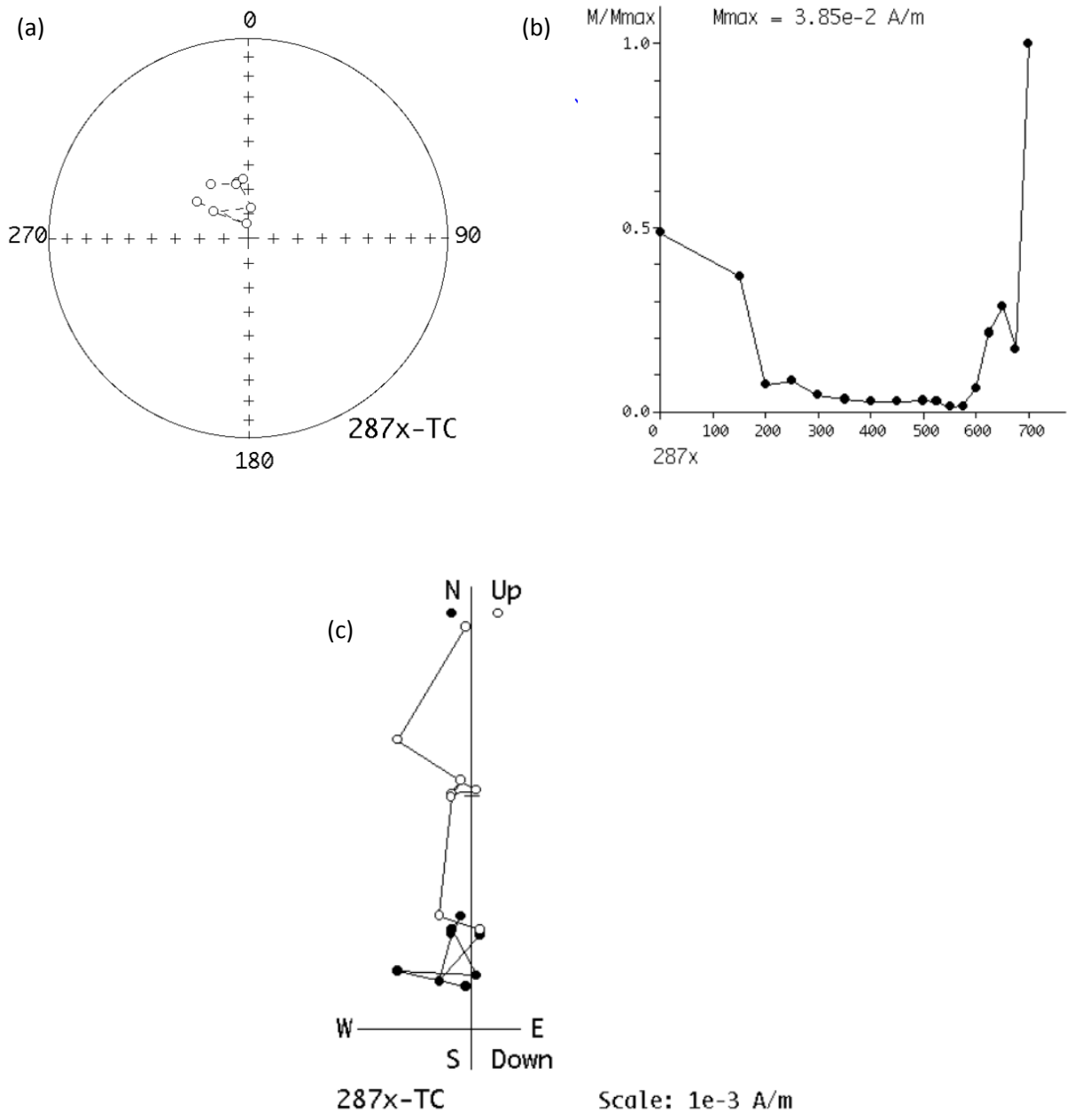

Figure 2: Demagnetization information for sample 287x from site 62 showing its (a) Stereonet plot of magnetic directions between temperature ranges of 250-550°C (b) Intensity diagram showing decay between 0-350°C due to a lower temperature component and 580°C indicative of the presence of low-titanium magnetite. Decay beyond 580°C is likely due to acquired magnetizations of new oxides introduced from oxidation of magnetite and (c) the corresponding Zijderveld diagram between 300-575°C that suggests the primary magnetic directions while secondary directions from lower-temperature components are noisy and not shown in the diagram. This sample is not used in the final paleopole calculation as it was the only individual sample in site 62 with α95 of <17°, thus disqualifying site 62.

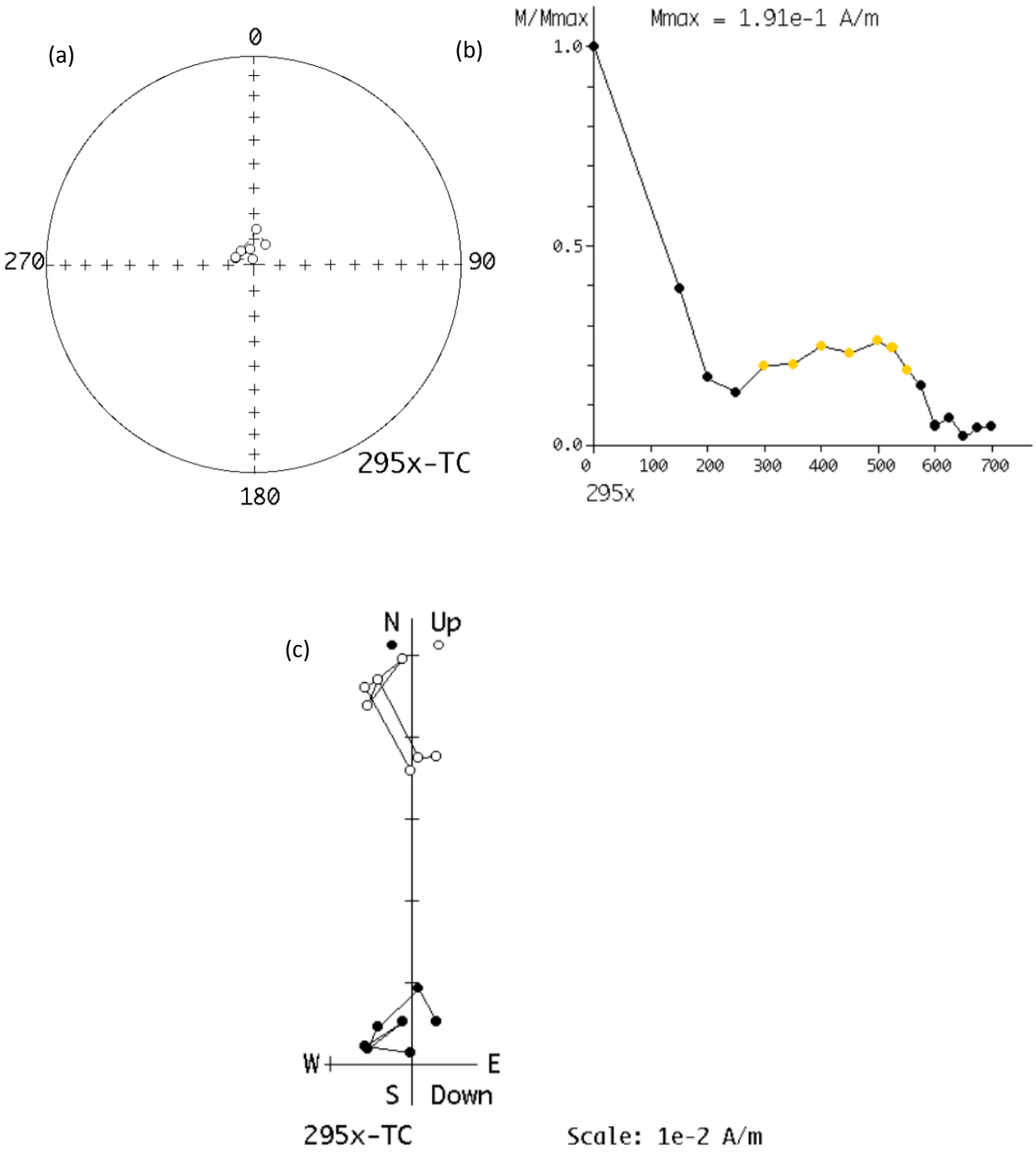

Figure 3: Demagnetization information for sample 295x from a different location (site 64) showing its (a) Stereonet plot of magnetic directions between temperature ranges of 300-575°C (b) Intensity diagram showing decay between 0-250°C due to a lower temperature component and 580°C indicative of the presence of low-titanium magnetite and (c) the corresponding Zijderveld diagram between 300-575°C that suggests the primary magnetic directions while secondary directions from lower-temperature components are noisy and not shown in the diagram. Directions are north-northwesterly and up. This sample was eliminated from calculation of site mean as the α95 of site 64 is smaller without sample 295x.

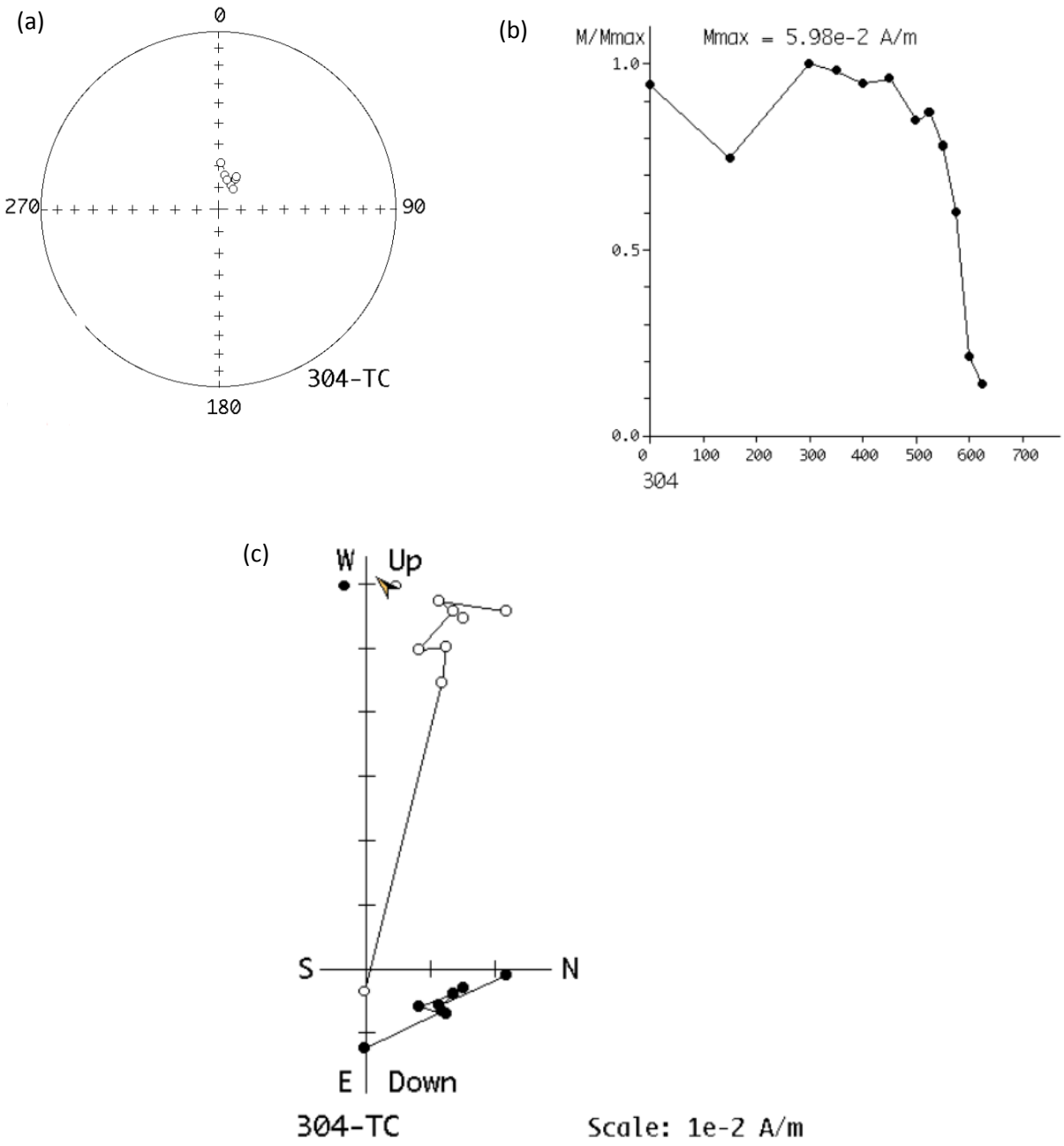

Figure 4: Demagnetization information for sample 304 from a different location (site 66) showing its (a) Stereonet plot of magnetic directions between temperature ranges of 300-575°C (b) Intensity diagram showing decay between 0-600°C due to a high-temperature component indicative of the presence of low-titanium magnetite and (c) the corresponding Zijderveld diagram between 300-550°C that suggests the primary magnetic directions. Demagnetization steps above 600°C suggests the presence of hematite, however directions are noisy and not shown in the diagram. Directions of cluster decay to the origin and are north-northeasterly and up.

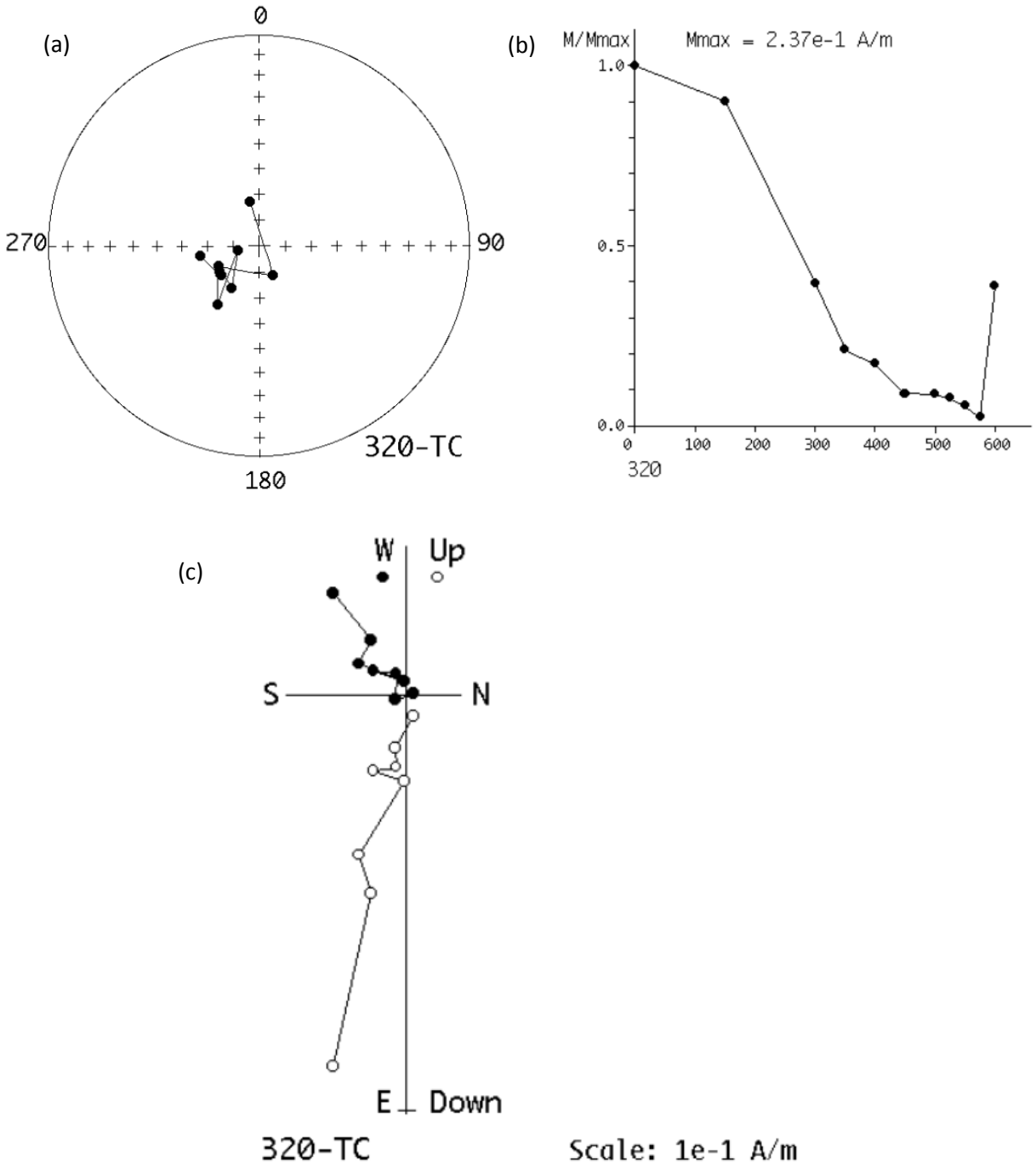

Figure 5: Demagnetization information for sample 320 from a different location (site 70) showing its (a) Stereonet plot of magnetic directions between temperature ranges of 0-575°C (b) Intensity diagram showing decay between 0-600°C due to a high-temperature component indicative of the presence of low-titanium magnetite and (c) the corresponding Zijderveld diagram between 350-575°C that suggests the primary magnetic directions. Demagnetization steps above 600°C are noisy and not shown in the diagram. Directions are southwesterly and down.

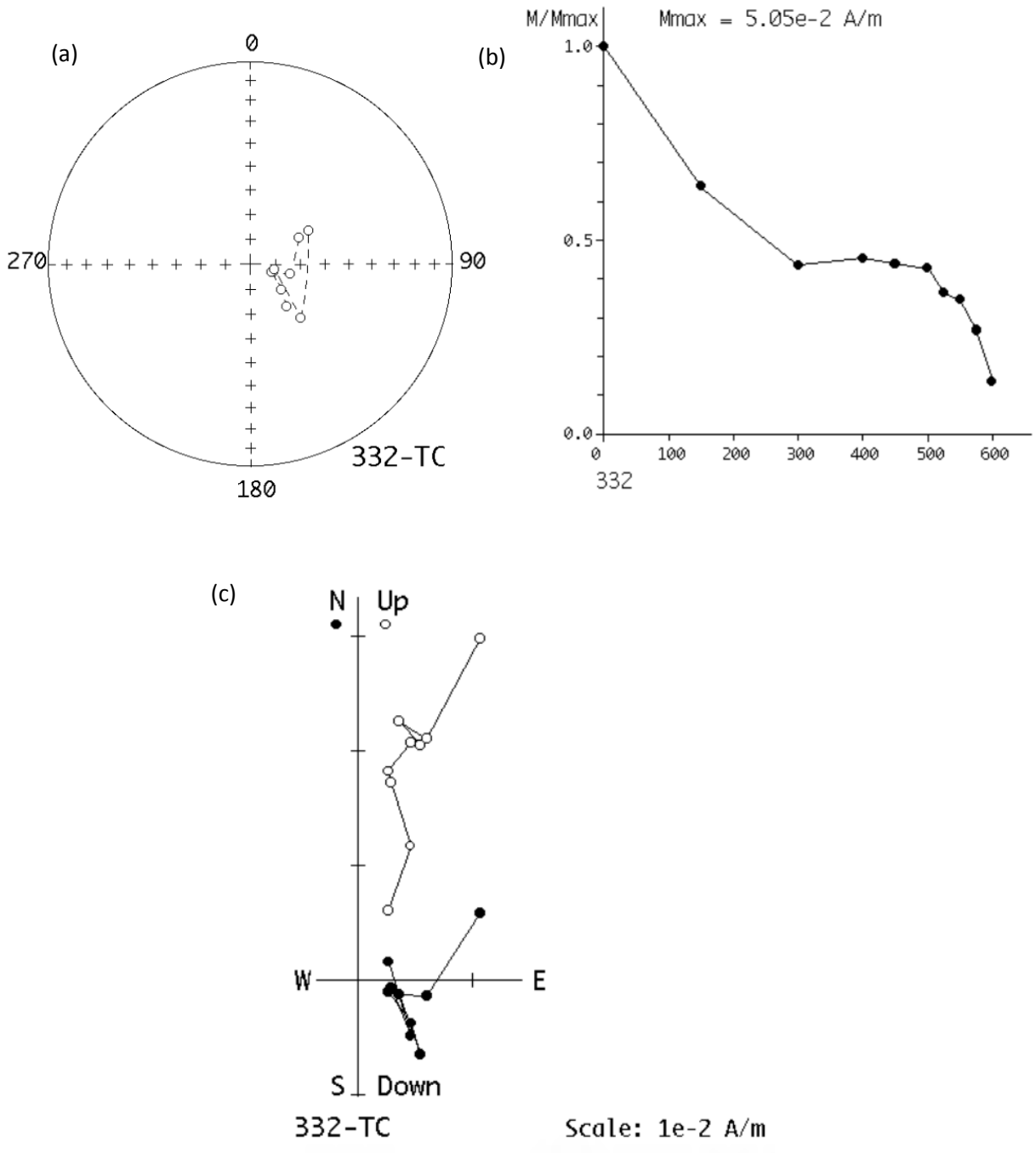

Figure 6: Demagnetization information for sample 332 from a different location (site 73) showing its (a) Stereonet plot of magnetic directions between temperature ranges of 0-600°C (b) Intensity diagram showing decay between 350-600°C due to a high-temperature component indicative of the presence of magnetite and (c) the corresponding Zijderveld diagram between 150-600°C that suggests the primary magnetic directions. Demagnetization steps above 600°C are noisy and not shown in the diagram. Directions are south-southeasterly and up.

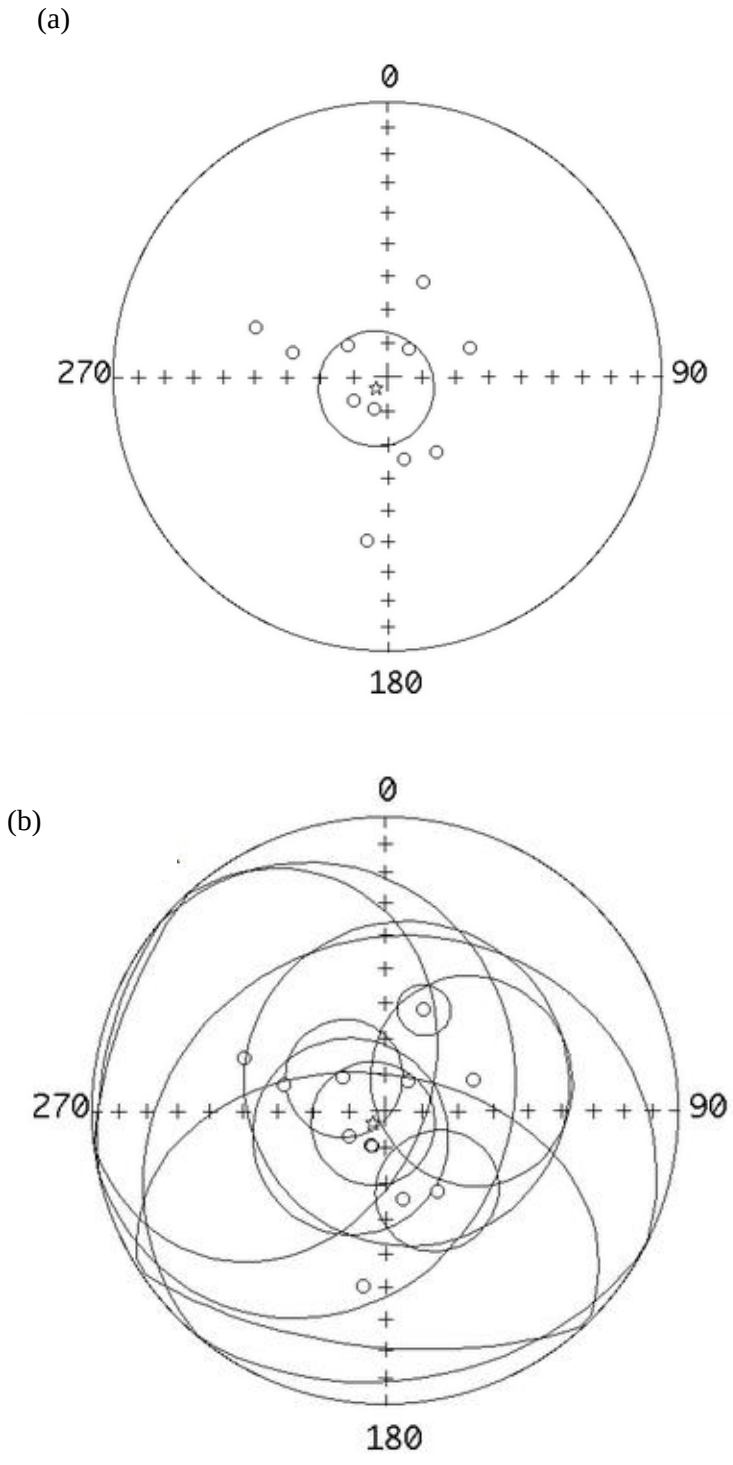

Figure 7: Final mean (represented by a star) computed from mean of sites yields a declination and inclination (tilt-corrected) of 181.7° and -86.6° respectively (a) mean of each sites are shown (b) mean of each sites are shown with the corresponding α95 values.

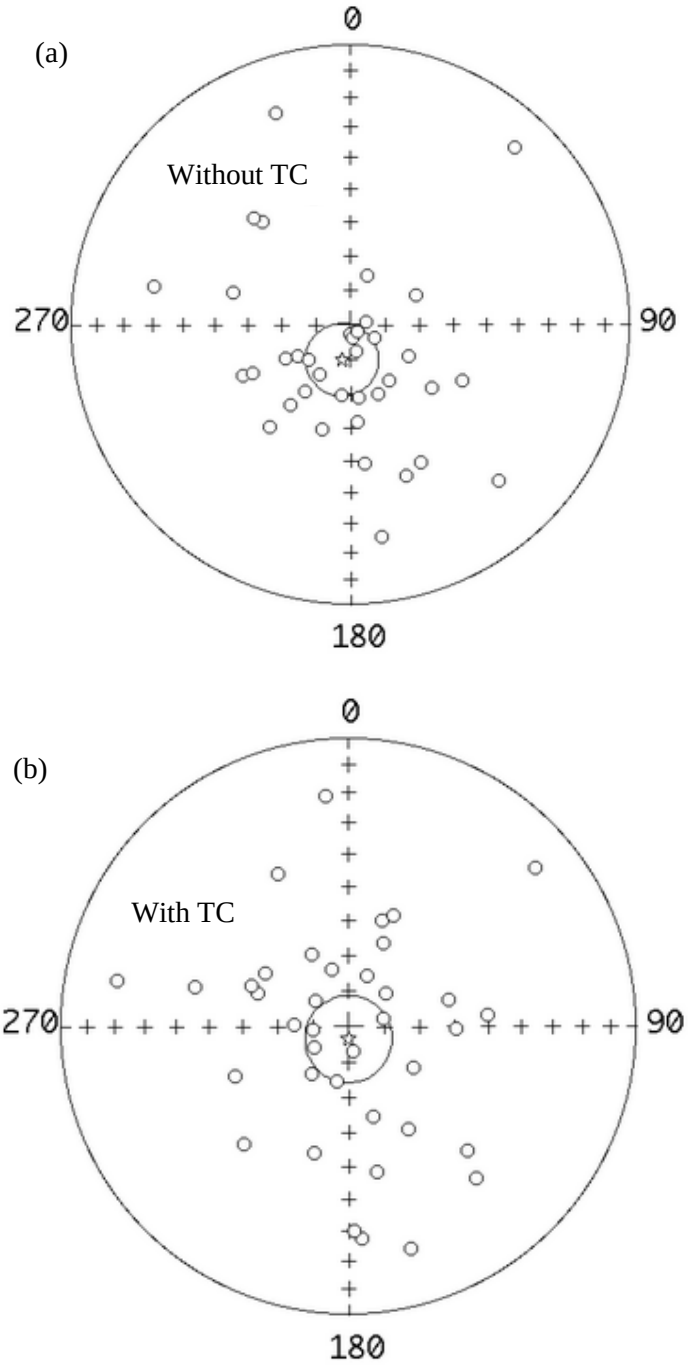

Figure 8: Two stereonets showing comparison between directions of samples (a) prior to bedding correction (b) after bedding correction. Corresponding k_1 and k_2 are found to be 5.8 and 4.6 respectively giving a k_2/ k_1 value of 0.79 and n=38 yielding a negative and inconclusive fold test at the 95% confidence level. Some sample directions have been inverted to be of the same polarity. TC: tilt-correction.

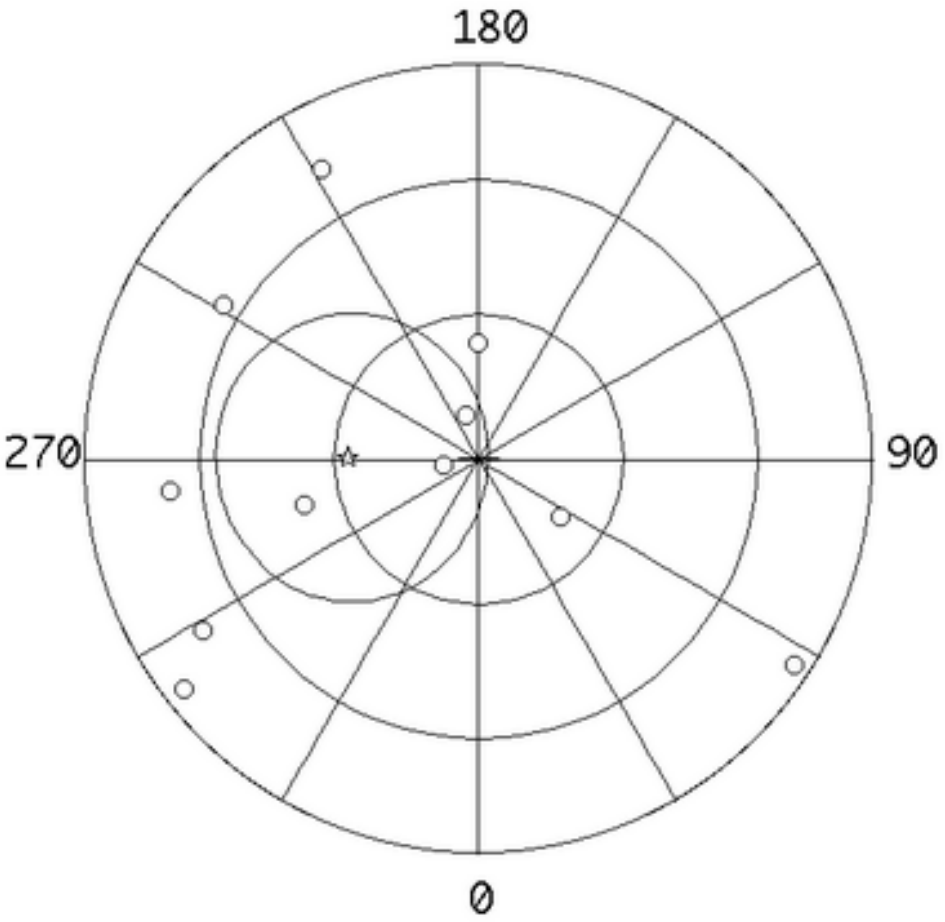

Figure 9: Orthographic projection showing tilt-corrected VGPs calculated from reliable sites. A paleopole of 268.8°, -83.2° is obtained with α95 of 28.2°. As per **Table 2**, 11 sites out of 16 were selected for analysis. To obtain the paleopole, only 8 sites out of the selected 11 were used to decrease the value of α95 to 28.2°.

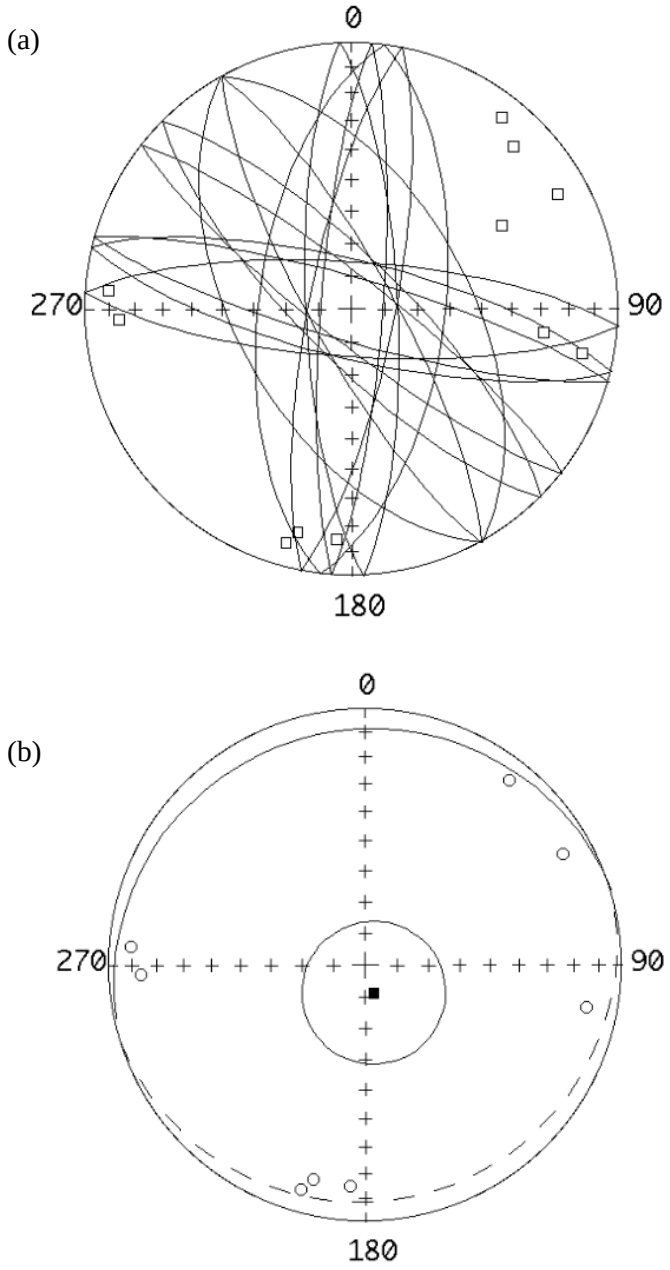

Figure 10: Two stereonets showing results of the Great Circle Analysis of the sites (a) planes that correspond to the magnetic direction of each site are portrayed in the upper hemisphere and open squares represent the normal to the planes (b) unreliable normal are eliminated through visual inspection and a great circle is fitted to the normal to obtain a common magnetic direction represented by the closed square.

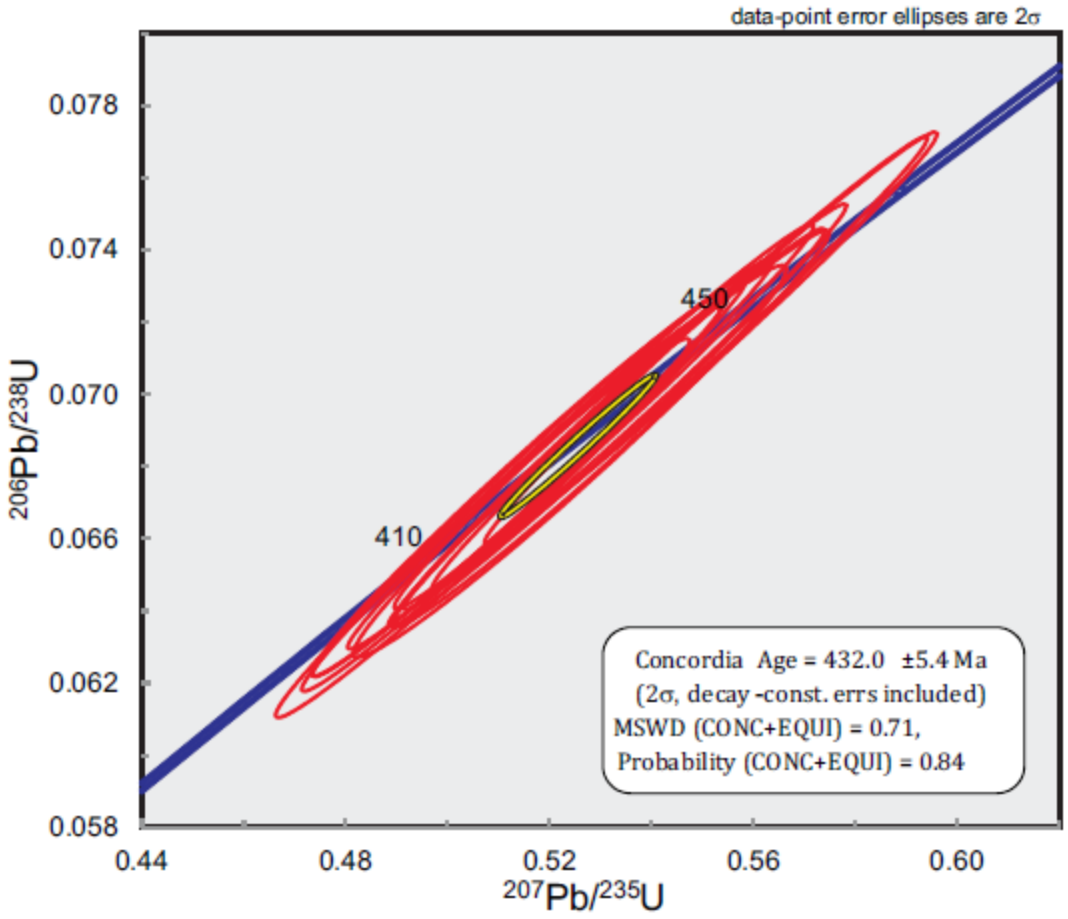

Figure 11: The diagram shows the Concordia for a U-Pb radiometric dating done on zircon from the samples. This analysis was done by Joe Meert (University of Florida) and the result was obtained through Prof. Van der Voo via personal communication. The samples from the study site are estimated to be of age 432.0 ± 5.4 Ma.

Table 1: Core information, organized by sample number, MAD angle (anchored or non-anchored, depending on the vector of the decay), core orientation, statistical parameters and magnetic directions. Declination correction of +5.2° not applied.

Sample	Site	MAD Angle	Core Dec.	Core Inc.	k	a95	n	Geo. Dec.	Geo. Inc.	Strat. Dec.	Strat. Inc.
291	63	12.5	66	27	29.7	17.1	4	136.6	-24.0	139.9	-31.9
292	63	11.7	2	27	213.4	9.9	4	239.4	-72.1	217.2	-73.2
293x	63	9.3	1	29	54.6	12.5	4	177.2	-87.3	264.4	-80.2
294	63	4.9	94	75	216.8	3.8	8	171.6	-24.5	176.3	-27.3
296	64	7.9	125	73	24.4	12.5	7	101.0	29.4	101.0	19.4
297	64	8.2	-4	41	68.8	6.7	8	19.7	-74.8	344.3	-73.4
298	64	8.2	35	38	68.6	15.0	3	285.4	-54.3	284.4	-44.3
303	66	7.2	95	80	132.8	6.1	7	127.7	-59.8	85.2	-49.7
304	66	4.4	2	46	308.9	3.4	7	229.3	-74.1	20.0	-74.9
305	66	7.1	-2	16	105.1	8.6	4	145.6	-70.2	75.0	-60.6
307	67	3.8	265	14	468.6	3.9	5	187.2	-69.4	167.8	-82.9
308	67	6.0	211	22	134.0	6.6	5	214.3	-66.4	237.4	-78.7
310	67	4.5	-35	54	231.0	6.3	5	171.9	-85.9	191.3	-74.0
315	69	7.5	-58	3	232.1	6.6	7	216.9	-60.6	307.5	-78.6
316	69	5.9	74	7	69.4	8.3	6	241.9	-68.6	333.3	-67.2
317	69	6.2	61	26	125.3	7.7	5	218.1	-51.4	271.1	-74.7
319	70	3.2	152	35	223.7	5.1	6	164.1	50.2	174.3	21.2
320	70	4.0	205	14	94.4	6.5	7	353.8	68.4	229.3	76.0
321	70	5.4	86	77	96.3	7.0	6	64.3	54.9	122.7	62.1
322	70	6.6	-65	64	64.2	8.8	6	332.8	43.9	271.6	59.1
323	71	16.6	5	72	18.6	16.0	6	355.6	61.4	257.7	79.7
324	71	7.4	-45	24	93.6	7.9	4	136.6	-86.9	17.5	-58.5
325	71	10.4	-60	22	41.8	9.4	7	81.3	-85.5	22.4	-56.0
326	71	3.0	-3	34	624.1	2.4	7	167.3	-82.1	22.8	-64.7
331	73	4.5	-60	1	268.0	4.0	6	119.2	-81.9	164.8	-63.4
332	73	9.2	99	35	69.3	6.9	9	66.4	-69.1	122.3	-68.0
333	73	14.6	104	30	23.6	13.0	7	118.5	-70.8	149.3	-56.0
334	73	7.3	-64	13	95.9	6.2	7	211.3	-72.8	194.7	-52.3
335	74	9.3	40	84	58.9	8.9	8	63.3	58.0	41.5	44.5
336	74	8.7	41	81	69.7	7.2	8	139.2	50.1	110.1	62.8
338	74	4.3	54	30	296.7	4.2	6	160.6	21.4	155.2	41.7
339x	75	2.3	-90	14	102.8	6.6	6	296.6	53.0	315.9	40.0
340x	75	2.2	246	11	190.9	5.6	5	337.9	68.2	348.7	47.2
341	75	11.9	14	52	34.3	11.9	6	222.9	15.0	229.7	16.3
342	75	6.3	252	44	142.9	5.1	7	137.9	47.5	112.4	60.3
344	76	12.6	225	69	23.4	16.8	5	174.0	-48.6	178.1	-29.5
345	76	14.7	121	66	36.5	16.2	5	159.5	-41.8	164.3	-21.0
346	76	5.8	-15	44	192.8	4.9	6	195.3	-58.3	246.2	-54.7

Table 2: General site information, organized by site number, sample range, statistical parameters, and VGP directions (N1: total number of samples collected; N2: number of treated samples; N3: number of samples used for analysis). na: site was not used in calculation for final pole. Declination correction of +5.2° not applied.

Site	Sample Range	N1	N2	N3	Dec	Inc	k	α95	GPS Lat.	GPS Long.	VGP Long.	VGP Lat.	dp	dm	Paleolat.
61	283-286	4	4	0	na	na	na	na	42.5730	72.5310	na	na	na	na	na
62	287-290	4	4	0	na	na	na	na	42.5730	72.5318	na	na	na	na	na
63	291-294	4	4	4	234.4	-77.7	85.9	27.3	42.5720	72.5310	284.7	-52.3	48.1	51.2	-66.4
64	295-298	4	4	2	290.5	-47.7	6.4	53.2	42.5710	72.5310	308.1	-5.7	45.1	69.3	-28.8
65	299-302	3	3	0	na	na	na	na	42.5700	72.5317	na	na	na	na	na
66	303-306	3	3	3	70.6	-63.8	19.6	28.7	42.5692	72.5322	208.4	-18.1	36.2	45.6	-45.5
67	307-310	3	3	3	201.2	-79.7	112.3	1.7	42.5688	72.5327	280.0	-82.8	3.2	3.3	-70.0
68	311-314	4	4	0	na	na	na	na	42.5677	72.5347	na	na	na	na	na
69	315-318	3	3	3	308.4	-75.2	57.9	16.3	42.5673	72.5352	275.9	-22.6	27.3	29.8	-62.1
70	319-322	4	4	4	37.4	-79.6	8.3	46.0	42.5669	72.5362	239.1	-25.7	83.8	87.8	-69.8
71	323-326	4	4	4	20.8	-59.8	294.7	7.2	42.5648	72.5377	236.9	4.7	8.2	10.9	-40.7
72	327-330	4	4	3	na	na	na	na	42.5638	72.5400	na	na	na	na	na
73	331-334	4	4	4	147.0	-63.4	54.5	16.9	42.5624	72.5413	179.7	-66.2	21.1	26.7	-45.0
74	335-338	4	4	3	283.9	-61.0	4.8	64.3	42.5606	72.5449	302.1	-18.8	75.4	98.5	-42.1
75	339-342	4	4	4	168.5	-65.0	3.8	74.4	42.5602	72.5455	195.0	-80.7	96.9	120.1	-47.0
76	343-346	4	4	3	187.0	-39.6	5.2	60.6	42.5592	72.5473	54.2	-69.1	43.6	72.7	-22.5

Table 3: Pre- and post-folding correction for tilted samples, yielding an inconclusive fold test (McElhinny, 1964). Samples with reverse polarity were inverted to normal polarity. Declination correction of +5.2° not applied. TC: tilt-correction.

			Without TC		*With TC*	
Sample	**n**	**a95**	**Geo Dec**	**Geo Inc**	**Strat Dec**	**Strat Inc**
291	4	17.1	136.6	-24.0	139.9	-31.9
292	4	9.9	239.4	-72.1	217.2	-73.2
293x	4	12.5	177.2	-87.3	264.4	-80.2
294	8	3.8	171.6	-24.5	176.3	-27.3
296	7	12.5	101.0	29.4	101.0	19.4
297	8	6.7	19.7	-74.8	344.3	-73.4
298	3	15.0	285.4	-54.3	284.4	-44.3
303	7	6.1	127.7	-59.8	85.2	-49.7
304	7	3.4	229.3	-74.1	20.0	-74.9
305	4	8.6	145.6	-70.2	75.0	-60.6
307	5	3.9	187.2	-69.4	167.8	-82.9
308	5	6.6	214.3	-66.4	237.4	-78.7
310	5	6.3	171.9	-85.9	191.3	-74.0
315	7	6.6	216.9	-60.6	307.5	-78.6
316	6	8.3	241.9	-68.6	333.3	-67.2
317	5	7.7	218.1	-51.4	271.1	-74.7
319	6	5.1	164.1	50.2	174.3	21.2
320	7	6.5	353.8	68.4	229.3	76.0
321	6	7.0	64.3	54.9	122.7	62.1
322	6	8.8	332.8	43.9	271.6	59.1
323	6	16.0	355.6	61.4	257.7	79.7
324	4	7.9	136.6	-86.9	17.5	-58.5
325	7	9.4	81.3	-85.5	22.4	-56.0
326	7	2.4	167.3	-82.1	22.8	-64.7
331	6	4.0	119.2	-81.9	164.8	-63.4
332	9	6.9	66.4	-69.1	122.3	-68.0
333	7	13.0	118.5	-70.8	149.3	-56.0
334	7	6.2	211.3	-72.8	194.7	-52.3
335	8	8.9	63.3	58.0	41.5	44.5
336	8	7.2	139.2	50.1	110.1	62.8
338	6	4.2	160.6	21.4	155.2	41.7
339x	6	6.6	296.6	53.0	315.9	40.0
340x	5	5.6	337.9	68.2	348.7	47.2
341	6	11.9	222.9	15.0	229.7	16.3
342	7	5.1	137.9	47.5	112.4	60.3
344	5	16.8	174.0	-48.6	178.1	-29.5
345	5	16.2	159.5	-41.8	164.3	-21.0
346	6	4.9	195.3	-58.3	246.2	-54.7

Mean

Without TC

Dec	**Inc**	**R**	**k1**	**a95**
194.2	-79.6	3.16E+01	5.8	10.6

With TC

Dec	**Inc**	**R**	**k2**	**a95**
181.7	-86.6	2.99E+01	4.6	12.3

Table 4: General site information, organized by site number, sample range, statistical parameters, and normal to the best-fit plane from each sites of the Great Circle Analysis, represented by <Dec, Inc>. na: site was not used in calculation for final pole. Declination correction of +5.2° not applied. Sites with asterisk were not used in computing the common magnetic direction for all sites.

Site	Sample Range	N1	N2	N3	Dec	Inc	α95	GPS Lat.	GPS Long.
61	283-286	4	4	0	na	na	na	42.5730	72.5310
62	287-290	4	4	0	na	na	na	42.5730	72.5230
63	291-294	4	4	4	60.9	-12.6	25.5	42.5720	72.5310
64	295-298	4	4	2	3.7	14.5	5.1	42.5710	72.5310
65	299-302	3	3	0	na	na	na	42.5700	72.5317
66	303-306	3	3	3	13.6	15.0	0.4	42.5692	72.5322
67	307-310	3	3	3	38.0	-9.9	40.2	42.5688	72.5327
68	311-314	4	4	0	na	na	na	42.5677	72.5347
69	315-318	3	3	3	280.9	13.2	14.4	42.5673	72.5352
70	319-322	4	4	4	15.7	9.8	4.0	42.5669	72.5362
71	323-326	4	4	4	94.3	9.5	6.5	42.5648	72.5377
72	327-330	4	4	3	na	na	na	42.5638	72.5400
73	331-334	4	4	4	267.5	-14.0	11.4	42.5624	72.5413
74*	335-338	4	4	3	276.8	28.6	3.7	42.5606	72.5449
75*	339-342	4	4	4	44.8	-15.3	17.0	42.5602	72.5455
76*	343-346	4	4	3	60.8	-35.7	3.9	42.5592	72.5473

Appendix

Sampling Localities: This appendix contains basic information on sites where samples are obtained. As a whole, the sites are volcanic rocks intertwined with conglomerates and sandstones. Most sites are flat-lying and measurements are taken with the Right-Hand Rule convention. Magnetic properties are measured for each flow using a Fluxgate Magnetometer (FM, unit: μT) and a Kappameter (K, unit: SI).

Site 61: Mafic volcanic rock with underlying sediments. Fine-grained rocks and turned brown due to weathering. Heading down-section, you will hit Pt. 15. ARG-61 collected.

Samples:	283-286
Location:	N 42.5730° E 72.5310°
K:	1.08
FM:	29.9
Strike:	10°
Dip:	10°

Site 62: Basaltic layer over Site 61. Similar characteristics with rocks in Site 61. ARG-61 collected.

Samples:	287-290
Location:	N 42.5729° E 72.5318°
K:	1.02
FM:	26.1
Strike:	10°
Dip:	10°

Site 63: Basaltic layer over Site 62. Similar characteristics with rocks in Site 62. ARG-63 collected.

Samples:	291-294
Location:	N 42.5720° E 72.5310°
K:	16.8
FM:	-21.3
Strike:	10°
Dip:	10°

Site 64: Basaltic layer over Site 63. Similar characteristics with rocks in Site 63, 62 and 61. ARG-64 collected.

Samples:	295-298
Location:	N 42.5710° E 72.5310°
K:	13.6
FM:	40.9
Strike:	10°
Dip:	10°

Site 65: Basaltic layer over Site 64. Similar characteristics with rocks in Site 64, 63, 62 and 61. ARG-65 collected. Different orientation from previous sites. Has overlying greenish sandstone.

Samples:	299-302
Location:	N 42.5700° E 72.5317°
K:	11.3

FM: 52.3
Strike: 125°
Dip: 30°

Site 66: Basaltic layer over the greenish sandstone that overlies Site 65. Similar characteristics with rocks in Site 64, 63, 62 and 61. ARG-66 collected.

Samples: 303-306
Location: N 42.5692° E 72.5322°
K: 6.43
FM: 76
Strike: 125°
Dip: 30°

Site 67: Basaltic layer over Site 66. Similar characteristics with rocks in Site 66. Non-vesicular. ARG-67 collected.

Samples: 307-310
Location: N 42.5687° E 72.5327°
K: 18.1
FM: 25.4
Strike: 105°
Dip: 14°

Site 68: Basaltic layer over Site 67. Similar characteristics with rocks in Site 67. There is a gap of about 250-400m between this and the previous site. Probably due to the green sandstone that has been washed away for being less resistant. ARG-68 collected.

Samples: 311-314
Location: N 42.5677° E 72.5347°
K: 4.77
FM: 39.8
Strike: 105°
Dip: 32°

Site 69: Basaltic layer over Site 68. Similar characteristics with rocks in Site 68. ARG-69 collected.

Samples: 315-318
Location: N 42.5672° E 72.5352°
K: 12.9
FM: 48.1
Strike: 105°
Dip: 32°

Site 70: Basaltic layer over Site 69. Slightly vesicular with 1-2mm diameter vesicles, non-flattened. Slightly greenish on some parts. ARG-70 collected.

Samples: 319-322
Location: N 42.5669° E 72.5362°
K: 17.4
FM: 21.5

Strike: 105°
Dip: 32°

Site 71: Basaltic layer over Site 70. Slightly more felsic, even andesitic. ARG-71 collected.

Samples: 323-326
Location: N 42.5648° E 72.5377°
K: 5.48
FM: 21.3
Strike: 105°
Dip: 32°

Site 72: Basaltic layer over Site 71. ~500m of sandstone and possibly other sediment (covered). Highly mafic and turns maroon to red when weathered. Fine-grained. ARG-72 collected.

Samples: 327-330
Location: N 42.5638° E 72.5400°
K: 19.9
FM: 33.0
Strike: 271°
Dip: 22°

Site 73: Thick basaltic layer over Site 72 and ~200m layer of sediment. Grey to black when fresh and maroon to brown when weathered. Slightly vesicular with ~1mm (diameter) vesicles. Fine-grained matrix with some elongate black crystals suspected to be hornblende. Overlain by a thin felsic flow, that wasn't sampled. ARG-73 collected.

Samples: 331-334
Location: N 42.5623° E 72.5413°
K: 6.66
FM: 34.5
Strike: 271°
Dip: 22°

Site 74: Very thick basaltic layer over Site 73 (~250m thick). Grey to black basalts overlying a thin siltstone layer (~1m thick). Medium-grained with some greenish patches and plagioclase crystals. ARG-74 collected.

Samples: 335-338
Location: N 42.5606° E 72.5449°
K: 3.83
FM: 26.2
Strike: 271°
Dip: 22°

Site 75: Very thick basaltic flow over Site 74. Contact between flows highly visible. Medium-grained matrix with plagioclase crystals present (smaller than the crystals found in Site 74). Black basalts and turns dark brown when weathered. ARG-75 collected.

Samples: 339-342
Location: N 42.5602° E 72.5455°

K: 18.3
FM: 34.5
Strike: 271°
Dip: 22°

Site 76: Intermediate (andesitic) flow and lies above Site 75. Medium-grained matric with abundant plagioclase crystals. Grey to black when fresh and beige to red when weathered. Slightly vesicular with vesicles of ~1mm diameter. ARG-76 collected.

Samples: 343-346
Location: N 42.5592° E 72.5473°
K: 3.32
FM: 36.8
Strike: 271°
Dip: 22°